JURNAL TEKNIK SIPIL CENDEKIA
e-ISSN:2723-3375
doi : 10.51988/jtsc.v7i2.525
pp : 361-370

Seismic Response and Liquefaction Control on Sloping Ground Using Groundwater Lowering Strategy

Rina Rebut Rayhansah[1*], Muhsiung Chang[2], Hsu-Jen Lin[3], Muhammad Hamzah Fansuri[4], Togani Cahyadi Upomo[5], Rini Kusumawardani[5]

[1]Dept of Civil Engineering, Faculty of Engrg, Universitas Kadiri, Kediri, Indonesia
[2]Dept of Civil and Construction Engrg, Nat'l Yunlin Univ of Sci & Tech, Yunlin, Taiwan, ROC
[3]Dept of Civil and Construction Engrg, Nat'l Yunlin Univ of Sci & Tech, Yunlin, Taiwan, ROC
[4]Dept of Civil Engrg, Universitas Pertahanan Republik Indonesia, West Java, Indonesia
[5]Dept of Civil Engrg, Universitas Negeri Semarang, Central Java, Indonesia

[*)]Correspondence writer rinarebutrayhansah@unik-kediri.ac.id

Received: 25 April 2026 Revised: 18 Mei 2026 Accepted: 27 Mei 2026

Abstract

Liquefaction-induced slope failure remains a critical geotechnical problem in seismic regions, particularly under saturated sloping ground conditions. This study investigates the effects of slope inclination and groundwater depth on liquefaction behavior using numerical simulation under seismic loading. Three slope configurations (i1–i3) and two groundwater conditions, W2 (3.84 m) and W3 (9 m), were analyzed to evaluate excess pore water pressure (EPP), seismic amplification, spectral response, and lateral deformation. Results show that steeper slopes and deeper groundwater conditions significantly modified soil dynamic behavior. Peak acceleration increased from 0.127 g under i1–W2 to 0.190 g under i3–W3, while the dominant spectral period shifted to T ≈ 1.443 s with maximum spectral acceleration reaching Sa,max ≈ 0.529 g. Groundwater lowering (GL) effectively reduced pore pressure generation and produced nearly drained conditions within the computational zone. However, the Encased Stone Column (ESC) system provided better performance in minimizing lateral deformation and liquefaction-induced flow displacement. These findings demonstrate that hydraulic control and reinforcement systems play complementary roles in improving the stability of liquefaction-prone sloping soils under earthquake loading.

Keywords: *Encased Stone; Groundwater Depth; Liquefaction; Seismic; Sloping Ground*

Abstrak

Kegagalan lereng akibat likuefaksi masih menjadi permasalahan geoteknik yang kritis di wilayah rawan gempa, khususnya pada kondisi tanah miring jenuh air. Penelitian ini menginvestigasi pengaruh kemiringan lereng dan kedalaman muka air tanah terhadap perilaku likuefaksi menggunakan simulasi numerik di bawah pembebanan gempa. Tiga konfigurasi lereng (i1–i3) dan dua kondisi muka air tanah, yaitu W2 (3,84 m) dan W3 (9 m), dianalisis untuk mengevaluasi excess pore water pressure (EPP), amplifikasi seismik, respons spektral, dan deformasi lateral. Hasil penelitian menunjukkan bahwa lereng yang lebih curam dan kondisi muka air tanah yang lebih dalam secara signifikan memodifikasi perilaku dinamis tanah. Percepatan puncak meningkat dari 0,127 g pada kondisi i1–W2 menjadi 0,190 g pada i3–W3, sedangkan periode spektral dominan bergeser hingga T ≈ 1,443 s dengan percepatan spektral maksimum mencapai Sa,max ≈ 0,529 g. Groundwater lowering (GL) efektif mengurangi pembentukan tekanan air pori dan menghasilkan kondisi hampir terdrainase pada zona komputasi.

Namun, sistem Encased Stone Column (ESC) menunjukkan kinerja yang lebih baik dalam meminimalkan deformasi lateral dan perpindahan aliran akibat likuefaksi. Temuan ini menunjukkan bahwa sistem pengendalian hidraulik dan perkuatan tanah memiliki peran komplementer dalam meningkatkan stabilitas tanah miring yang rentan terhadap likuefaksi akibat gempa.

Kata kunci: *Encased Stone; Kedalaman Muka Air Tanah; Likuefaksi; Amplifikasi Seismik; Lereng Miring*

INTRODUCTION

Soil liquefaction drastically reduces slope stability, causing severe structural displacement and catastrophic earthquake-induced infrastructure collapse globally [1], [2], [3], [4], [5], [6], [7]. The 1999 recorded over 90% structural collapse dominated by progressive slope reduction failures [8] (Fig. 1). Indonesia experienced devastating liquefaction-induced flowslides during the 2018 , particularly within densely populated Petobo regions [9], [10], [11], [12]. Limited understanding regarding liquefaction-area bearing capacity under sloping conditions still threatens long-term structural foundation safety significantly [13], [14].

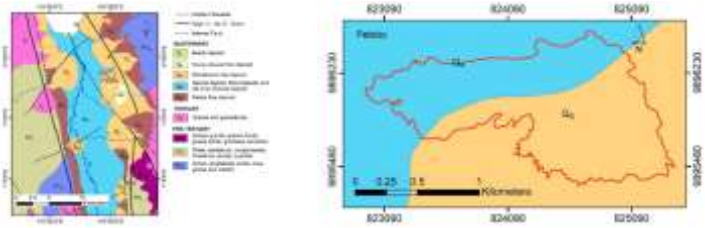

(a) (b)

Figure 1. (a) Geological Map of Palu (Hanifa 2018); (b) the red line indicates the Petobo research area which is composed of alluvial deposits and debris (Kusumawardani 2021)
Source:[15]

Groundwater lowering strategies significantly improve sloping soil stability, yet empirical liquefaction studies remain critically limited globally [1], [2]. Most previous studies emphasized arid regions, creating adaptation difficulties for vulnerable soft coastal liquefaction-prone soil conditions [3], [4], [5], [6]. Black-box predictive models frequently ignore mechanistic soil behavior, despite groundwater reduction strongly influencing lateral deformation stability [7], [8], [9]. Integrated slope-based liquefaction mitigation research remains urgently required to overcome conventional drainage system performance limitations effectively [10], [11].

Soil liquefaction transforms saturated ground into fluid-like material during earthquakes structures[28], [29], [30]. Modern mitigation prioritizes non-disruptive methods and advancing multidisciplinary innovations[20], [24], [31], [32].Vertical drains rapidly dissipate excess pore pressures underground[16], [18], [33].Maintained effective stress prevents liquefaction and damage[24], [29]. Groundwater lowers crust thickness and reduces liquefaction effects[16], [34]. Capillary stress increases strength and improves safety[35], [36]. Liquefaction slope damages houses; drainage and piles reduce risks[37]. In 1995 Kobe earthquake, Tsukiji houses collapsed; groundwater lowered 1.5–2 m, filled 1.5 m soil, forming stable 3–3.5 m crust[34](Fig. 1; Table 1).

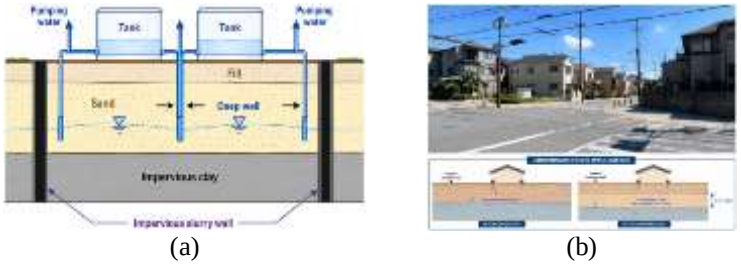

(a) (b)

Figure 2. (a) Lowering ground water level for mitigation[34]; (b) Tsukiji area of Amagasaki city where ground water level was lower[34]

Table1. Related Works

No	Author's	Pore Mechanics	Drainage Model	Stability	Analysis Method	Findings	Weakness

1	[16]	v			Centrifuge and FEM simulations	Unsaturated soils showed higher seismic stability.	Excluded flat residential liquefaction conditions.
2	[18]	v			Clay FEM modeling	Saturation controls uplift reduction effectiveness.	Black-box models ignored physical soil mechanisms.
4	[19]		v		Groundwater computational modeling	GWL prediction reached NSE 0.94–0.96.	Required massive metropolitan stratigraphic datasets.
6	[17]	v			Vadose zone simulations	Thick vadose zones stabilized water flux.	Limited only to arid soil conditions.
7	[20]	v		v	Soft sand stabilization simulations	Lower water increased shear strength significantly.	Laboratory scale lacked seismic validation testing.
8	[21]		v		Groundwater fluctuation simulations	Stable extraction maintained at 50 m spacing.	Geotechnical behavior received limited investigation focus.

This study offers a mapping of soil response due to the Groundwater Lowering (GL) strategy influenced by slope variations. Unlike previous studies, which focused on flat land, this simulation hypothesizes that increasing groundwater depth to 9 m (W3) reduces the pore water pressure ratio to zero in the 7 m critical zone, even though the slope slope triggers lateral deformation (18.05 cm). The study contributes to new design parameters that demonstrate the superior effectiveness of GL in controlling pore pressure that requires structural support from Encased Stone Columns (ESC) to mitigate optimal lateral ground movement.

METHOD

This study applied 3D OpenSeesPL simulations evaluating liquefaction mitigation under nonlinear static-seismic loading conditions [38]. [39]. Six scenarios combined groundwater depths W2–W3 with slope inclinations i1–i3 systematically for comprehensive seismic evaluation [32], [40], [41]. Groundwater depths reached 3.84–9 meters, while slopes varied between 0° and 6° continuously simulated [42], [43] [44], [45], [46]. Scaled CHY002 earthquake acceleration reached 0.308g using DEEPSOIL before OpenSeesPL seismic input application [28], [47] (Fig. 3).

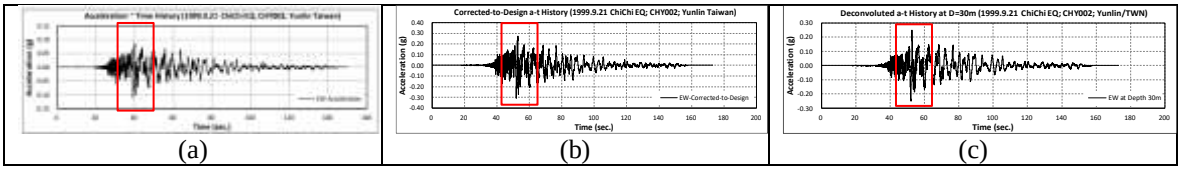

(a) (b) (c)

Figure 3. (a) Earthquake acceleration time history (1999.9.21 ChiChi EQ; CHY002; EW, PGA=0.110g); (b) Earthquake acceleration time history modified to the design PGA of 0.308g (1999.9.21 ChiChi EQ; CHY002; EW, PGA=0.308g); (c) Deconvoluted acceleration time history at 30 m deep adopted as the input motion for current OpenSeesPL analysis (1999.9.21 ChiChi EQ; CHY002; EW, PGA=0.249g)

OpenSeesPL simulations evaluate groundwater lowering effectiveness mitigating liquefaction-induced flowslides in three-dimensional soils[38], [48]. CRAFD groundwater levels change coseismically, requiring approximately 250 days for recovery[22]. CRAFD groundwater dipped 250 days before; 78% stations rose coseismically significantly[49]. Groundwater lowering was evaluated for liquefaction mitigation using 620 elements and 896 nodes. Models included varying groundwater depths with 3 different ground inclinations[34], [37](Fig. 4; Table 2; Table 3).

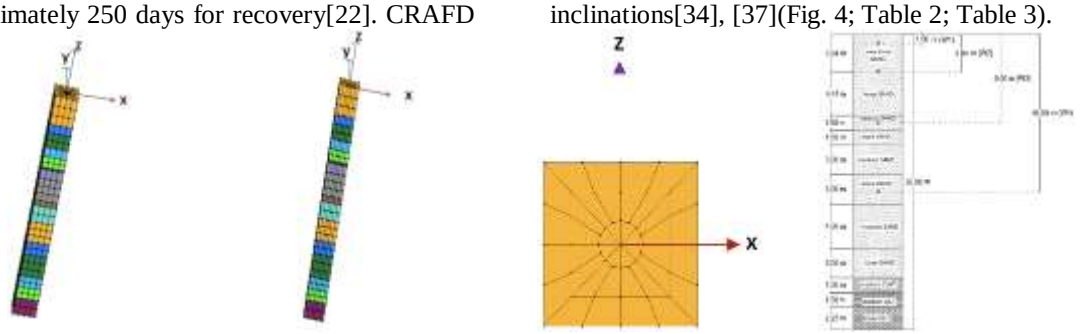

(a) (b) (c) (d)

Figure 4. (a) 3D full mesh of GL; (b) 3D half mesh of GL; (c) 3D Top Mesh of GL; (d) A cross section of Groundwater lowering in Soil Properties

Table 2. Analysis framework for geosynthetic-encased stone column (ESC)

Analysis No.	Diameter d (m) [d1, d2, d3] [0.4, 0.8, 1.2]	Spacing s (m) [s1, s2, s3] [1.4, 2.8, 4.2]	Thickness of Geosyn t (m) [t1, t2, t3] [1E-3, 5E-3, 9E-3]	Length L (m) [L1, L2, L3, L4] [4.5, 9, 18, 27]	Ground inclination i (deg.) [i1, i2, i3] [0, 3, 6]
ESCd2s2t2L4il*), i2*), i3*)	0.8	2.8	5.00E-03	27	0, 3, 6

Note: *indicates duplicated cases and OG for Original
Level of replacement ratio (Rr; %) is 1.6~25.66
Permeability of stone column (kSC; m/s) is 0.01
Permeability of geosynthetic-encased stone column (kgeosyn; m/s) is 0.001

Table 3. Analysis framework for Groundwater Lowering (GL)

Analysis No.		GW Depth ; W (m)	i (degrees)
GL W2	i1	16	0
	i2	1	3
	i3	3.84	6
GL W3	i1	9	0
	i2	16	3
	i3	1	6

Note: GW – Groundwater Lowering
W – Depth of groundwater lowering [W2 = 3.84 m; W3 = 9 m].
i – Ground Inclination [i1 = 0 deg; i2 = 3 deg; i3 = 6 deg]

RESULTS AND DISCUSSION

Numerical simulation evaluates groundwater lowering at depths 1m 3.84m 9m and slopes 0°, 3°, 6°. Groundwater lowering prevents excess pore pressure using W1 W2 W3 conditions effectively observed. For W2 depth 3.84m GL equals original ground condition across all inclinations exactly. Excess pore pressure ratio reaches 1.0 indicating liquefaction at W2 while W3 zero. Steeper slope increases displacement yet slightly reduces excess pore pressure response overall value. Encased stone column outperforms groundwater lowering reducing liquefaction and lateral deformation most effectively.

a. Excess pore pressure plots (Center of soil model)

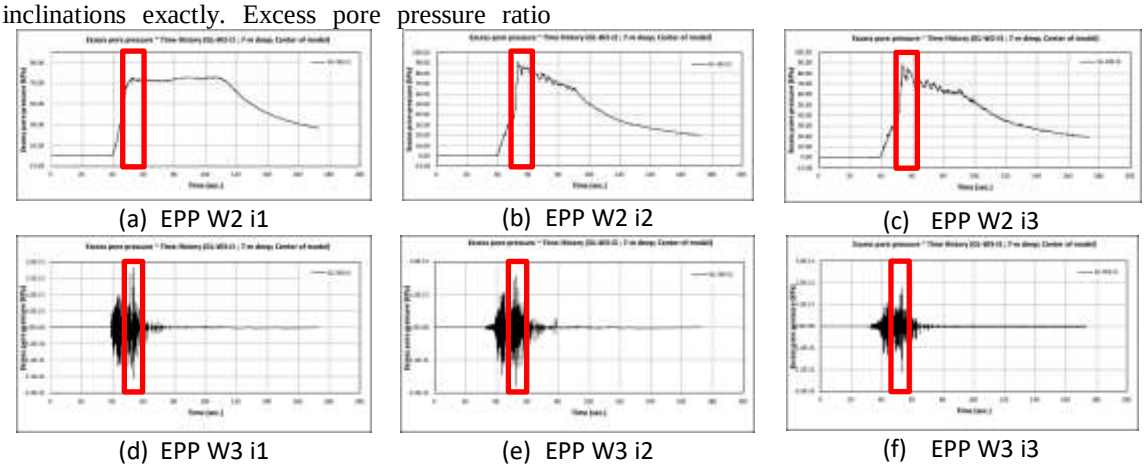

Figure 5. Excess pore pressure plots (Center of soil model) W2 & W3 [W2 = 3.84 m; W3 = 9m]; [i1 = 0 deg; i2 = 3 deg; i3 = 6 deg]

Note:
Excess pore water pressure = EPP

b. Acceleration time history

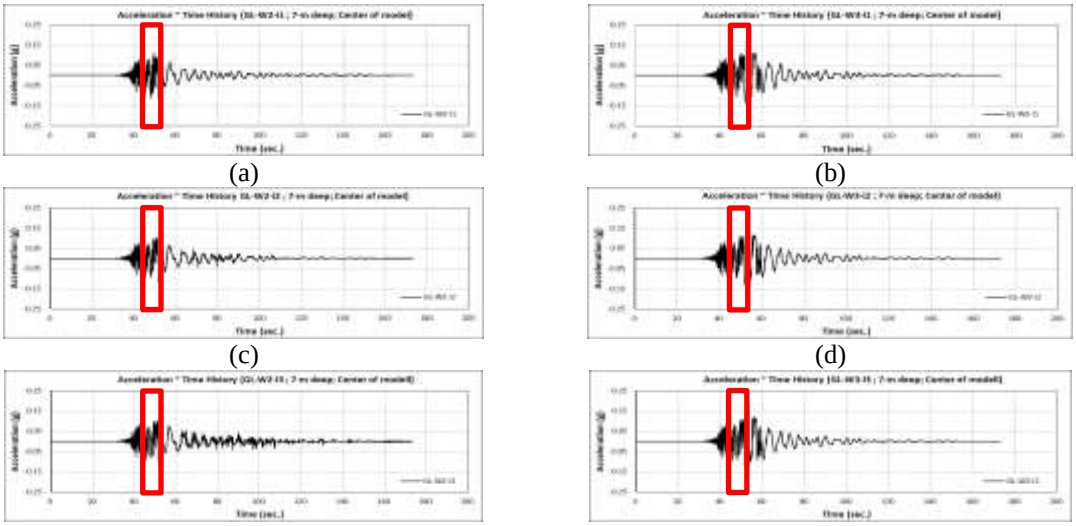

Figure 6. (a) Acceleration time history of 0 deg. (OG-i1) and Groundwater Table (W2) 3.84 m of SC at 7-m deep for soils at the center of model (Amax = 0.127 g); (b) Acceleration time history of 0 deg. (OG-i1) and Groundwater Table (W3) 9 m of SC at 7-m deep for soils at the center of model (Amax = 0.170 g; (c) Acceleration time history of 3 deg. (OG-i2) and Groundwater Table (W2) 3.84 m of SC at 7-m deep for soils at the center of model (Amax = 0.163 g); (d) Acceleration time history of 3 deg. (OG-i2) and Groundwater Table (W3) 9 m of SC at 7-m deep for soils at the center of the model (Amax = 182 g); of 6 deg. (OG-i3) and Groundwater Table (W3) 9 m of SC at 7-m deep for soils at the center of model (Amax = 0.190 g)

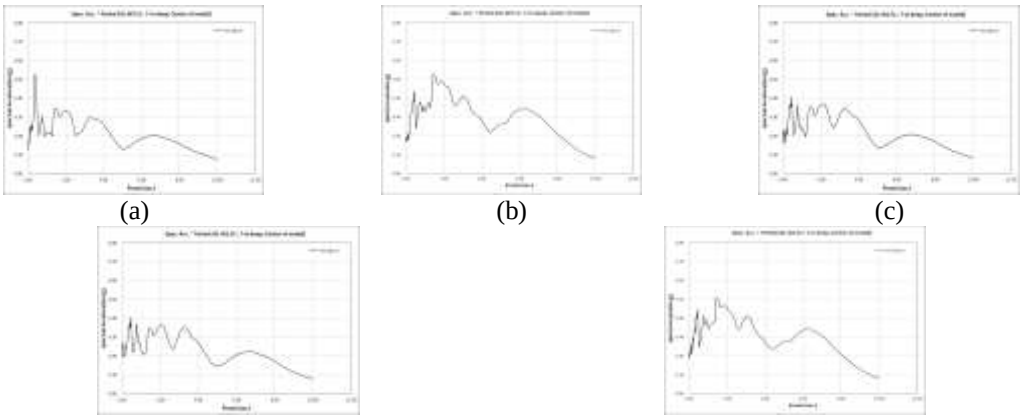

Figure 7. (a) Acceleration response spectra (5% damping) of 0 deg. and Groundwater Table (W2) 3.84 m of SC at 7-m deep for soils at the center of model (Sa, max =0.527g and T=0.368sec.; (b) Acceleration response spectra (5% damping) of 0 deg. and Groundwater Table (W3) 9 m of SC at 7-m deep for soils at the center of model (Sa, max =0.529g and T=1.443sec.); (c) Acceleration response spectra (5% damping) of 3 deg at 7-m deep for soils at the center of model (Sa, max =0.406g and T=0.471sec.); e) Acceleration response spectra (5% damping) of 6 deg. and Groundwater Table (W3) 9 m of SC at 7-m deep for soils at the center of model (Sa, max =0.511g and T=1.443sec.)

model)

c. Displacement time history plots (Center of soil

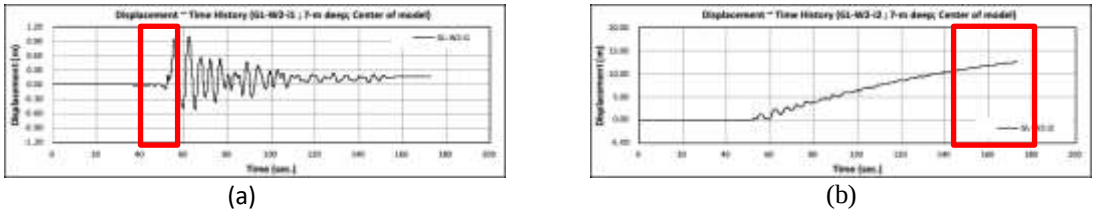

(c) (d)

Figure 8. Displacement time history plots (Center of soil model) [W2 = 3.84 m]; [i1 = 0 deg; i2 = 3 deg; i3 = 6 deg]

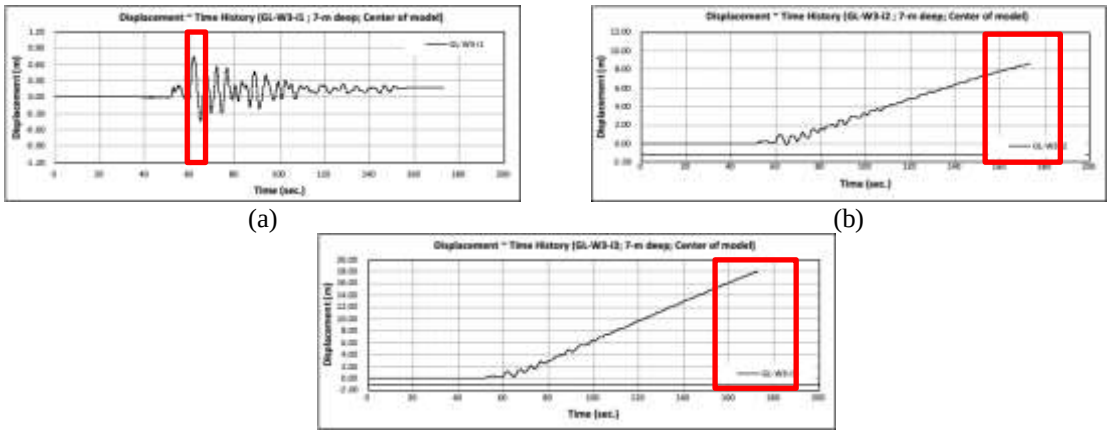

(a) (b)

(c)

Figure 9. Displacement time history plots (Center of soil model) [W3 = 9 m]; [i1 = 0 deg; i2 = 3 deg; i3 = 6 deg]

d. Displacement profile plots (Center of soil model)

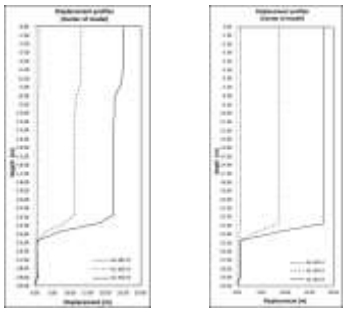

(a) (b)

Figure 10. (a) Displacement profile plots (Center of soil model) W2 [i1 = 0 deg; i2 = 3 deg; i3 = 6 deg]; (b) Displacement profile plots (Center of soil model) W3 [i1 = 0 deg; i2 = 3 deg; i3 = 6 deg]

Numerical simulations reveal strong interactions between groundwater depth, slope inclination, and seismic intensity at the model center. Fig. 5(a)–(f) shows W2 (3.84 m) produces more controlled EPP responses than W3 (9 m), where deeper saturation generates broader pressure distribution and higher fluctuation amplitudes.

Fig. 6(a)–(f) indicates deeper groundwater does not consistently reduce seismic response. Peak acceleration increases from 0.127 g (i1–W2) to 0.170 g (i1–W3), reaching 0.190 g under i3–W3, suggesting stronger amplification on steeper slopes.

Spectral responses in Fig. 7(a)–(e) demonstrate W3 shifts dominant periods toward longer ranges (T ≈ 1.443 s) compared with W2 (T ≈ 0.368–0.471 s). Spectral acceleration also increases significantly up to Sa,max ≈ 0.529 g, indicating altered dynamic soil behavior under deeper saturation.

Deformation analysis from Fig. 8–Fig. 10 confirms W3 combined with steeper slopes (i2–i3) generates larger cumulative displacement and wider lateral deformation zones. In contrast, W2 produces more localized deformation patterns with lower displacement continuity.

Integrated results from Fig. 5–Fig. 10 confirm groundwater depth does not linearly improve stability. Instead, deeper groundwater significantly modifies pore pressure distribution, seismic amplification, and deformation mechanisms under inclined ground conditions.

The groundwater lowering (GL) scenario using

W3 (9 m), positioned below the critical computational depth of 7 m, effectively suppresses excess pore pressure generation and produces nearly drained conditions during seismic loading. This mechanism reduces soil–water interaction and decreases liquefaction susceptibility within the computational zone. However, despite its effectiveness in reducing pore pressure, GL alone shows limitations in controlling lateral spreading and cumulative deformation under sloping ground conditions.

In comparison, the Encased Stone Column (ESC) system demonstrates superior and more stable performance in mitigating liquefaction-induced deformation. Unlike GL, which primarily modifies hydraulic conditions, ESC simultaneously increases soil stiffness, confinement, drainage capacity, and shear resistance. As a result, ESC not only reduces excess pore pressure generation but also significantly limits lateral displacement and flow deformation under seismic loading. The reinforcement effect provided by the geosynthetic encasement improves load transfer mechanisms and restrains soil movement more effectively, particularly under steeper slope configurations. Therefore, while GL is effective as a hydraulic mitigation strategy, ESC provides a more comprehensive seismic ground improvement solution for liquefaction-prone sloping soils because it combines drainage enhancement with structural reinforcement against deformation and instability.

Table 4. Originality

Dimensions	Specific Findings	Key	Originality
Interaction	Certain slope inclinations reduce $((i)\Delta u/\sigma'_v)$ at specific depths.	$i = 0° \rightarrow 6°$	Slope inclination does not always intensify all seismic response parameters.
Mitigation Depth Threshold	W3 (9 m) reduced excess pore pressure to zero at 7 m depth.	$\Delta u/\sigma'_v = 0$	Critical pump depth identified for eliminating liquefaction risk in vulnerable zones.
Lateral vs Vertical Efficiency	GL eliminated pore pressure, but lateral deformation remained higher than ESC	Max Dis W2 : 24.9 vs Max Dis W3 : 18	GL requires ESC integration for effective lateral deformation control performance.
Correlation of Frequency and Acceleration	Groundwater depth significantly altered Response Spectra and dominant vibration periods.	T $= 0.368s \rightarrow 1.443s$	Dewatering shifts natural vibration periods through effective stress modification.

CONCLUSION

Groundwater depth significantly alters excess pore pressure, acceleration, spectral response, and deformation behavior. W3 condition increases peak acceleration up to 0.190 g compared with W2. Deeper groundwater shifts the dominant period toward 1,443 seconds, indicating stronger dynamic amplification effects. Slope inclination intensifies response variability under both W2 and W3 conditions significantly. Design strategies must consider groundwater depth effects since deeper conditions may amplify seismic response. Ground improvement approaches should prioritize combined hydraulic and mechanical mitigation rather than single control measures. Future studies should investigate coupled hydro-mechanical interactions under varying soil layering and heterogeneity conditions. Advanced probabilistic seismic modeling is recommended to capture uncertainty in groundwater-driven dynamic soil response.

ACKNOWLEDGEMENT

Research funding through MOST, Taiwan, with Project No. MOST-110-2221-E-224-054 is gratefully appreciated. Muhammad Hamzah Fansuri for technical suggestions and technical support during the numerical analysis. Special thanks are owed to Prof. Muhsiung Chang.

REFERENCES

[1] AG Papadimitriou, AI Valsamis, and TG Limnaiou, “Liquefaction mitigation methods for existing shallow-founded elongated structures on horizontal or mildly-inclined ground,”*Soil Dyn. Earthq. Eng.*, vol. 162, no. August, p. 107453, 2022, doi: 10.1016/j.soildyn.2022.107453.

[2] Y. Miyata, “Geosynthetic MSE walls research and practice: past, present, and future (2023 IGS Bathurst Lecture),”*Geosynth. Int.*, vol. 32, no. 1, pp. 62–81, 2024, doi: 10.1680/jgein.24.00054.

[3] WS Chen*et al.*, “1999 Chi-Chi earthquake: A case study on the role of thrust-ramp structures for generating earthquakes,” Bull. Seismol. Soc. Am., vol. 91, no. 5, pp. 986–994, 2001, doi: 10.1785/0120000731.

[4] D. Forcellini, “Soil-structure interaction analyzes of shallow-founded structures on a potential-liquefiable soil deposit,”*Soil Dyn. Earthq. Eng.*, vol. 133, no. March, p. 106108, 2020, doi: 10.1016/j.soildyn.2020.106108.

[5] JS Rajeswari and R. Sarkar, "Adequacy of batter piles under seismic conditions: A review of past performances and investigations,"*Structures*, vol. 61, no. February, p. 106022, 2024, doi: 10.1016/j.istruc.2024.106022.

[6] A. Tohari, D. Dani Wardhana, M. Hanif, and K. Koizumi, "Understanding of subsurface conditions controlling flow liquefaction occurrence during the 2018 Palu earthquake based on resistivity profiles,"*E3S Web Conf.*, vol. 331, p. 03002, 2021, doi: 10.1051/e3sconf/202133103002.

[7] R. Kusumawardani, M. Chang, TC Upomo, RC Huang, MH Fansuri, and GA Prayitno, “Understanding of Petobo liquefaction flowslide by 2018.09.28 Palu-Donggala Indonesia earthquake based on site reconnaissance,”*Landslides*, vol. 18, no. 9, pp. 3163–3182, 2021, doi: 10.1007/s10346-021-01700-x.

[8] AD Nugraha, F. Muttaqy, RV Ry, P. Supendi, and S. Rosalia, "Seismic velocity structure beneath the source region of the 2019 Ambon earthquake (Mw 6. 5), Indonesia, from local earthquake tomography,"*Earth, Planets Sp.*, pp. 1–14, 2026.

[9] M. Adib, M. Roesyanto, and S. Erwin, “AXIAL BEARING CAPACITY ANALYSIS OF 60 CM DIAMETER HYDRAULIC COMPRESSION PILE USING AXIAL STATIC LOAD TEST AND USING FINITE ELEMENT METHOD IN TOWER-1 INPATIENT BUILDING PROJECT OF HAJI HOSPITAL MEDAN (BASED ON BH-3 DATA),”*J. Civil Engineering Scholar*, vol. 6, no. 2, pp. 198–206, 2025, doi: 10.51988/jtsc.v6i2.304.

[10] L. Joko, P. Lucky, and A. Schipper, “INCREASING AIRCRAFT SERVICE CAPACITY (CASE STUDY OF TANJUNG WARUKIN AIRPORT, SOUTH KALIMANTAN),”*J. Civil Engineering Scholar*, vol. 1, no. 1, pp. 27–45, 2020.

[11] MV Kaisar and S. Erwin, “AXIAL BEARING CAPACITY ANALYSIS OF 60 CM DIAMETER PILE USING AXIAL STATIC LOAD TEST AND USING FINITE ELEMENT METHOD IN THE TOWER-1 INPATIENT BUILDING PROJECT OF HAJI HOSPITAL MEDAN,”*J. Civil Engineering Scholar*, vol. 6, no. 2, pp. 187–197, 2025, doi: 10.51988/jtsc.v6i2.303.

[12] AA Chandra, “MODIFICATION OF PLASTICITY PROPERTIES OF CLAY SOIL BY ADDITION OF SAND,”*J. Civil Engineering Scholar*, pp. 437–449, 2025.

[13] DP Vidya, R. Virtriana, I. Meilano, R. Raharja, M. Nabil, and A. Attar, "Taxonomy-driven exposure mapping for earthquake risk assessment in the active tectonic setting of Eastern Indonesia,"*Geoenvironmental Disasters*, 2026.

[14] MG Rachman and AA Shah, "Satellite image-based structural mapping reveals new earthquake sources in eastern Indonesia : implications for active tectonics and earthquake hazards,"*Natural hazards*, pp. 1–27, 2026.

[15] R. Kusumawardani, M. Chang, TC Upomo, and FL Caballero, "A regional site response analysis of the Petobo area after the 2018 .09 .28 Palu – Donggala Indonesia earthquake using an equivalent - linear model,"*Geoenvironmental Disasters*, 2025, doi: 10.1186/s40677-025-00308-w.

[16] SHS Jayakody, R. Uzuoka, and K. Ueda, “Effect of groundwater dynamics in rain-induced landslides: centrifuge and numerical study,”*Soils Found.*, vol. 64, no. 4, p. 101482, 2024, doi: 10.1016/j.sandf.2024.101482.

[17] L. Wu*et al.*, “Observation-constrained long-term simulations of water dynamics and groundwater recharge under intensive agriculture in the North China Plain,” Groundw. Sustain. Dev., vol. 31, no. September, p. 101516, 2025, doi: 10.1016/j.gsd.2025.101516.

[18] W. Sun, H. liu, W. Zhang, S. liu, and L. Han, “Determination of groundwater buoyancy reduction coefficient in clay: Model tests, numerical simulations and machine learning methods,”*Undergr. Sp.*, vol. 13, pp. 228–240, 2023, doi: 10.1016/j.undsp.2023.06.001.

[19] Y. Dai*et al.*, “Interpretable knowledge-driven framework for groundwater regime simulation: Integrating physical laws and graph-based reasoning for regional groundwater management,” J. Hydrol. Reg.

Stud., vol. 65, no. March, p. 103427, 2026, doi: 10.1016/j.ejrh.2026.103427.

[20] TT Doan, "Numerical simulation of the composite sand ground 'RHACLSMC' strains under the groundwater level and natural condition variations,"*Results Eng.*, vol. 26, no. April, p. 104991, 2025, doi: 10.1016/j.rineng.2025.104991.

[21] T. Sezer, AK Sani, RM Singh, L. Cui, DP Boon, and M. Woods, "Numerical investigation of a district scale groundwater heat pump system: A case study from Colchester, UK,"*Appl. Therm. Eng.*, vol. 236, no. PE, p. 121915, 2024, doi: 10.1016/j.applthermaleng.2023.121915.

[22] CH Chen*et al.*, "Anomalous frequency characteristics of groundwater levels before major earthquakes in Taiwan," Hydrol. Earth Syst. Sci., vol. 17, no. 5, pp. 1693–1703, 2013, doi: 10.5194/hess-17-1693-2013.

[23] Q. Wang, P. Geng, C. Chen, J. Chen, and C. He, "Determination of seismic response of reinforced tunnel portal slope using shaking table tests,"*Tunn. Undergr. Sp. Technol.*, vol. 136, no. February, p. 105072, 2023, doi: 10.1016/j.tust.2023.105072.

[24] X. Bao, Z. Jin, H. Cui, X. Chen, and X. Xie, "Soil liquefaction mitigation in geotechnical engineering: An overview of recently developed methods,"*Soil Dyn. Earthq. Eng.*, vol. 120, no. January, pp. 273–291, 2019, doi: 10.1016/j.soildyn.2019.01.020.

[25] M. Chang, C. ping Kuo, S. hui Shau, and R. eeh Hsu, "Comparison of SPT-N-based analysis methods in evaluation of liquefaction potential during the 1999 Chi-chi earthquake in Taiwan,"*Comput. Geotech.*, vol. 38, no. 3, pp. 393–406, 2011, doi: 10.1016/j.compgeo.2011.01.003.

[26] K. Nakai, I. Khan, and T. Noda, "Experiments and elastoplastic analyzes on soil disturbance of soft clay subjected to cyclic loading,"*Can. Geotech. J.*, pp. 1–15, 2026, doi: 10.1139/cgj-2025-0284.

[27] Y. Sun, C. Li, and D. Jin, "A novel nonlinear model for liquefaction potential assessment of stone column-improved ground incorporating multiple factors,"*Soil Dyn. Earthq. Eng.*, vol. 201, no. November 2025, p. 109966, 2026, doi: 10.1016/j.soildyn.2025.109966.

[28] Y. Huang, Z. Wen, L. Wang, and C. Zhu, "Centrifuge testing of liquefaction mitigation effectiveness on sand foundations treated with nanoparticles,"*Eng. Geol.*, vol. 249, no. January, pp. 249–256, 2019, doi: 10.1016/j.enggeo.2019.01.005.

[29] C. Yuan, Y. Pan, and S. Jing, "Simulation of soil water-salt dynamics and groundwater depth of spring maize based on SWAP model in salinized irrigation district,"*Comput. Electron. Agric.*, vol. 231, no. December 2024, p. 109992, 2025, doi: 10.1016/j.compag.2025.109992.

[30] S. Kollet*et al.*, "Global groundwater modeling: Proof-of-concept of 3D variably saturated flow simulation at kilometer resolution," J. Hydrol. X, vol. 30, no. December 2025, p. 100213, 2026, doi: 10.1016/j.hydroa.2025.100213.

[31] Y. Huang, Y. Yang, and J. Li, "Numerical simulation of artificial groundwater recharge for controlling land subsidence,"*KSCE J. Civ. Eng.*, vol. 19, no. 2, pp. 418–426, 2015, doi: 10.1007/s12205-015-0505-y.

[32] M. Pirone*et al.*, "Study of the groundwater regime in unsaturated slopes prone to landslides by multidisciplinary investigations: Experimental study and numerical modeling," Eng. Geol., vol. 315, no. November 2022, p. 107045, 2023, doi: 10.1016/j.enggeo.2023.107045.

[33] H. Bahadori, R. Farzalizadeh, A. Barghi, and A. Hasheminezhad, "A comparative study between gravel and rubber drainage columns for mitigation of liquefaction hazards,"*J. Rock Mech. Geotech. Eng.*, vol. 10, no. 5, pp. 924–934, 2018, doi: 10.1016/j.jrmge.2018.03.008.

[34] I. Towhata and R. Rasouli, "Attempts to protect personal houses from seismic liquefaction problems,"*Proc., 4th Int. Semin. Forensic Geotech. Eng.*, no. January 2013, pp. 191–209, 2013.

[35] Z. Safarzadeh and MH Aminfar, "Experimental and numerical modeling of the effect of groundwater table lowering on bearing capacity of shallow square footings,"*Int. J. Eng. Trans. A Basics*, vol. 32, no. 10, pp. 1429–1436, 2019, doi: 10.5829/ije.2019.32.10a.12.

[36] Y. Zhao, H. Wang, J. Wang, Y. Yang, X. Dong, and Z. Ma, "Study on regional nonlinear seepage flow combining indoor tests and numerical simulation,"*J. Hydrol. Reg. Stud.*, vol. 64, no. September 2025, p. 103157, 2026, doi: 10.1016/j.ejrh.2026.103157.

[37] R. Rasouli, I. Towhata, H. Rattez, and R. Vonaesch, "Mitigation of Nonuniform Settlement of Structures due to Seismic Liquefaction,"*J. Geotech. Geoenvironmental Eng.*, vol. 144, no. 11, pp. 1–10, 2018, doi: 10.1061/(asce)gt.1943-

5606.0001974.

[38] J. Lu, A. Elgamal, Z. Yang, and S. Diego, "OpenSeesPL : 3D Lateral Pile-Ground Interaction Jinchi Lu , Ahmed Elgamal , and Zhaohui Yang University of California , San Diego Department of Structural Engineering December 2011," no. December, 2011.

[39] J. Ye, SM Mojtabaei, I. Hajirasouliha, and K. Pilakoutas, "Efficient design of cold-formed steel bolted-moment connections for earthquake resistant frames,"*Thin-Walled Structure.*, no. October, p. 105926, 2019, doi: 10.1016/j.tws.2018.12.015.

[40] L. Li, D. Huang, F. Jin, and S. Du, "Evaluation of synthetic and recorded ground motions for soil liquefaction analyses,"*Soil Dyn. Earthq. Eng.*, vol. 149, no. May, p. 106815, 2021, doi: 10.1016/j.soildyn.2021.106815.

[41] G. Sang, RJ Lunn, JM Minto, and G. El Mountassir, "Microbially induced carbonate precipitation for soil improvement: Insights from a meter-scale radial grouting trial,"*Biogeotechnics*, vol. 4, no. 1, p. 100157, 2026, doi: 10.1016/j.bgtech.2024.100157.

[42] KY Monique*et al.*, "Numerical simulation of the protection perimeters of groundwater catchment structures in crystalline bedrock environments: Case of the Babo watershed (Central-Western Côte d'Ivoire)," J. Hydrol. Reg. Stud., vol. 64, no. March 2025, 2026, doi: 10.1016/j.ejrh.2026.103231.

[43] J. Li, J. Wei, F. Gao, J. Lou, G. Yuan, and X. Wang, "Experimental investigation on filtration-viscosity coupling and reinforcement mechanisms of high-pressure splitting grouting in soft coal,"*Results Eng.*, vol. 30, no. February, p. 110253, 2026, doi: 10.1016/j.rineng.2026.110253.

[44] S. Demir and PT Özener, "Parametric investigation of effectiveness of high modulus columns in liquefaction mitigation,"*Soil Dyn. Earthq. Eng.*, vol. 139, no. June, 2020, doi: 10.1016/j.soildyn.2020.106337.

[45] A. Asgari, M. Oliaei, and M. Bagheri, "Numerical simulation of improvement of a liquefiable soil layer using stone column and pile-pinning techniques,"*Soil Dyn. Earthq. Eng.*, vol. 51, pp. 77–96, 2013, doi: 10.1016/j.soildyn.2013.04.006.

[46] MH Fansuri*et al.*, "Effects of various factors on behaviors of piles and foundation soils due to seismic shaking," Solid Earth Sci., vol. 7, no. 4, pp. 252–267, 2022, doi: 10.1016/j.sesci.2022.09.001.

[47] M. Zhao, G. Liu, C. Zhang, W. Guo, and Q. Luo, "State-of-the-art of colloidal silica-based soil liquefaction mitigation: An emerging technique for ground improvement,"*Appl. Sci.*, vol. 10, no. 1, 2020, doi: 10.3390/app10010015.

[48] A. Elgamal, J. Lu, Z. Yang, and T. Shantz, "Scenario-focused three-dimensional computational modeling in geomechanics,"*4th Int. Young Geotech. Eng. Conf.*, 2009.

[49] CH Chen*et al.*, "Groundwater-strain coupling before the 1999 Mw 7.6 Taiwan Chi-Chi earthquake," J. Hydrol., vol. 524, no. May, pp. 378–384, 2015, doi: 10.1016/j.jhydrol.2015.03.006.